NASA Technical Memorandum 82596

Nonlinear Laminate Analysis for Metal Matrix Fiber Composites

C. C. Chamis and J. H. Sinclair
Lewis Research Center
Cleveland, Ohio

Prepared for the
Twenty-second Structures, Structural Dynamics and Materials Conference
cosponsored by the AIAA, ASME, ASCE, and AHS
Atlanta, Georgia, April 6-8, 1981

NASA

NONLINEAR LAMINATE ANALYSIS FOR METAL MATRIX FIBER COMPOSITES

by C. C. Chamis* and J. H. Sinclair**

National Aeronautics and Space Administration
Lewis Research Center
Cleveland, Ohio 44135

SUMMARY

A nonlinear laminate analysis is described for predicting the mechanical behavior (stress-strain relationships) of angleplied laminates in which the matrix is strained nonlinearly by both the residual stress and the mechanical load and in which additional nonlinearities are induced due to progressive fiber fractures and ply relative rotations. The nonlinear laminate analysis (NLA) is based on linear composite mechanics and a piece-wise linear laminate analysis to handle the nonlinear responses. Results obtained by using this nonlinear analysis on boron-fiber/aluminum-matrix angleplied laminates agree well with experimental data. The results shown illustrate the in situ ply stress-strain behavior and synergistic strength enhancement.

E-763

INTRODUCTION

Metal matrix composites, especially boron-fiber/aluminum matrix, have been investigated intensively in recent years and are now considered seriously for use in aerospace structures (Refs. 1 and 2). Predicting the mechanical behavior and structural response of components fabricated from metal matrix composites requires use of various mathematical models. These models, for example, relate stresses to applied forces, stress intensities at the tips of cracks to nominal stresses, buckling resistance to applied force, and/or vibration response to excitation forces. The Models just mentioned require initial tangent and strain-dependent stress-strain relationships. Experimental data indicate that the stress-strain curves of unidirectional composites are: (1) slightly nonlinear along the fiber direction near fracture; (2) mildly nonlinear transverse to fiber direction; and (3) extensively nonlinear in intralaminar (in-plane) shear. In addition, analysis of experimental data shows that the lamination residual stresses (the fabrication process induces thermal strains) may be of sufficiently high magnitude to strain the aluminum matrix nonlinearly in certain ply orientation configurations (Refs. 3 to 5). When the matrix is strained nonlinearly, the stress-strain relationships of the laminate may become load-path dependent. Though the nonlinear response of composite behavior has received some attention (Refs. 5 to 7), the lamination residual strain nonlinearity, including its effects on subsequent loading, has not been examined. It is the purpose of tnis investigation to describe a nonlinear laminate analysis for predicting the nonlinear mechanical behavior (stress-strain relationships) of angleplied laminates in which the matrix is strained nonlinearly by both tne residual stress and the mechanical load.

*Aerospace and Composites Structures Engineer, Member AIAA.
**Aerospace Materials Engineer.
Both members of the Structures and Mechanical Technologies Division.

The nonlinear laminate analysis (NLA) is an approximate analysis. It consists of linear composite mechanics and a piece-wise linear laminate analysis to handle the nonlinear response of the in situ matrix and individual fiber fractures. The NLA, as used in the investigated described herein, has no programmed provisions for the automatic detection of laminate fracture. This provision will be incorporated in the near future.

THEORETICAL BASIS

The computational procedure developed for the nonlinear laminate analysis (NLA) of boron/aluminum angleplied laminates is approximate. It consists of linear composite micromechanics and piece-wise linear laminate analysis to handle the cumulative effects of the nonlinear response of the in situ matrix. Briefly, tangent properties of the current cumulative matrix strain level are used to compute ply properties using composite micromechanics. These ply properties are then used to determine laminate properties using linear laminate theory. The load is incremented and the ply stresses/strains are calculated using linear laminate analysis and the previous increment laminate and ply properties. The ply stresses and strains are used to calculate matrix strains in conjunction with ply and matrix previous increment properties. The matrix strains thus calculated are amplified using integrated matrix magnification factors (Ref. 5). The amplified strains are added to the cumulative strains and the matrix tangent properties are determined using "table look-up" for the next load increment. At this point also the percent of fibers fractured, if any, is determined and is used to modify the longitudinal ply properties.

The residual stresses due to a temperature difference between processing and use temperature are determined in slightly different way. The macro- and micro-residual strains are calculated using linear composite mechanics and average matrix thermal and mechanical properties. These average properties are used as inputs at the micromechanics analysis level to obtain the ply properties. The ply properties and the temperature difference between processing and use-temperatures are used as inputs as the laminate analysis level to compute the residual strains and stresses in the plies. The integrated residual strains in the matrix are computed using the ply strains and the strain magnification factors (Ref. 5). This approach predicted results which were in good agreement with measured data for initial tangent properties (Ref. 5).

Two key assumptions form the basis for the development of this NLA. These are: (1) the in situ matrix is nonlinearly orthoropic; and (2) the orthotropic properties associated with each strain component are independent and can be determined from table look-up of normal and shear stress-strain data. These assumptions introduce some approximations in the stress-strain relationships (constitutive relationships) of the in situ matrix. However, these approximations are thought to be minimal and, therefore, to have negligible effect on the results because of: (1) the in situ matrix is highly restrained by the proximity of the fibers and no flow rule in the "classical plasticity sense" is operative; (2) the relatively large magnitude of microresidual stresses in the matrix and (3) and most important, force equilibrium and strain compatibility are automatically satisfied individually and collectively at both the micromechanics and macromechanics levels.

The computational procedure for NLA is by necessity in the form of a computer program. In the present investigation, the computer program was

generated by modifying an available computer program (Ref. 8). This program consists of a collection of functional modules (routines) which carry out composite micromechanics, macromechanics, and laminate theory. The inputs to this computer program are constituent material properties, laminate configuration, and composite geometry.

A qualitative flow chart of the resulting computer program is shown in Fig. 1. The temperature difference is an input. Note the provision to check the positive definite condition of the array of the stress-strain relations of the aluminum matrix. Violation of this condition leads to predictions of negative moduli of elasticity for both the ply and the composite. The asterisk indicates where the initial tangent properties for the laminate are determined.

It can be seen in the flow chart that the NLA procedure is "tangent-marching." That is, the laminate response at the next load increment is predicting using previous increment tangent properties without local iteration (predictor but not corrector). Local iteration added only to the increased accuracy of the results but not to the conceptual formal structure of the NLA procedure. Besides, local iteration (predictor corrector approach) can readily be incorporated as needed.

The NLA used in the present investigation has several important features when compared with other approaches. These are: (1) composite micromechanics is used to describe the matrix nonlinear behavior; (2) progressive fiber fractures are tracked at the micromechanics level; (3) initial or residual strains are determined prior to mechanical load application; (4) development of suitable expressions for the approximate representation of the interfiber matrix strain variation; and (5) generally orthotropic nonlinear behavior of the in situ matrix is permitted for both initial strains and subsequent mechanical loadings. The main advantages of this approach are: (1) computer running time economy, (2) ease of input data preparation, (3) measured nonlinear stress-strain data for the ply under combined load is not required, and (4) the three-dimensional tangent properties for both ply and composite are computed routinely as a part of the analysis.

As was mentioned in the introduction this NLA does not have provisions for automatically detecting fracture of the laminate. This is determined by the user from the ply stress or strain states and/or from the execessively large strains of the laminate.

INPUT/OUTPUT

The input data required for the nonlinear computational procedure consists of tabular data of matrix thermal properties, stress-strain data due to mechanical load, and percent of fibers fractured due to mechanical load. The thermal data of the matrix was obtained from Ref. 9 and are shown in Table 1.

The mechanical load stress-strain data were obtained from axial tension and from torsion tests on thin tubes made from 6061-O aluminum. Briefly, the tube test section was 2 inches inside diameter, 10 inches long, and 0.060 inch in wall thickness. The tube was machined to the test section dimensions from commercial tube stock allowing 1 inch at each end for gripping. The tubes were instrumented at their midlength with strain gage rosettes. The tubes were loaded in a multiaxial testing machine under tension and torsion loads. Load and strain data were recorded at regular load intervals. These data were reduced to engineering stress-strain data using

a strain-gage data-reduction program (Ref. 10). Tensile load data suitable for input into the computational procedure are shown in Table 2. The corresponding shear data are shown in Table 3. The data for percent of fibers fractured was obtained from Ref. 11 and is summarized in Table 4.

Additional input data required include boron fiber material properties, composite geometry laminate configuration, load and load increment, temperature difference, and the correlation coefficients described in Ref. 8. The fiber properties used were: modulus = 57×10^6 psi, Poisson's ratio = 0.2, and thermal coefficient of expansion = 2.8×10^{-6} in/in°F. This input data set is general for boron/aluminum angleplied laminates with boron fiber in 6061-0 aluminum alloy.

A large amount of information is generated during the solution processes and printed out in addition to the input data. This information consists of the following general sets: (1) All the input data is printed out in table form for ease of cross checking and reference; (2) The results of the lamination residual stresses are printed out. These results include ply stresses and strains, matrix stresses and strains, and matrix moduli and Poisson's ratios corresponding to the residual stress/strain; (3) First load increment results are printed for initial tangent moduli and Poisson's ratios for both the ply and the laminate (Ref. 5); (4) Any or each load increment results are printed at user request. These results include ply and laminate tangent properties for that load increment and cumulative properties up to that load increment. All these results are printed out automatically at the last load increment; (5) Final cumulative results are printed after the last load increment. These are in table form listed at each load increment and include ply stresses and strains, ply equivalent matrix strain, ply relative rotation, laminate stresses and strains and laminate geometry changes for length, width and thickness. The final cumulative results can be used to plot nonlinear stress-strain curves for the laminate, in situ ply stress-strain curves, ply stress/strain influence coefficients and interply relative rotation. Some of these will be illustrated later in the discussion of results.

RESULTS, COMPARISONS AND DISCUSSION

The nonlinear laminate analysis (NLA) described previously was used to predict the stress-strain behavior of boron/aluminum (B/A) angleplied laminate (APL) with generic laminate configuration $[0_2/\pm\theta]_s$ loaded in tension at various angles to the 0° ply direction. The laminates were made from 4-mil diameter boron fiber in a 6061-0 aluminum alloy. The fiber volume ratio was about 0.50. The laminate fabrication and experimental program to generate the data are described in detail (Refs. 3 to 5).

The temperature difference used in the residual strain computations in this investigation was 700° F. The reason for this choice is that the matrix starts supporting stress greater than 1000 psi between 800° and 700° F (Table 1). Also, this temperature difference was used to predict the initial tangent properties (Ref. 5), which correlated with measured data. The load at fracture was applied to the laminate in twenty equal increments. The computer running time was about 4 seconds for the twenty increments in the UNIVAC 1110.

NLA results are compared with measured data in Fig. 2, for a unidirectional laminate loaded 0°, 10°, and 90° to the fiber direction. The results plotted are laminate stress versus laminate strain. The agreement is excellent except for the final strain in the 10° off-axis specimen. Part of

this difficulty may be due to the extrapolation method that is used to determine the measured strain at fracture (Ref. 10). The results in Fig. 2 show that unidirectional boron/aluminum laminates exhibit: (1) mild nonlinearity when loaded parallel (longitudinal) or perpendicular (transverse) to the fiber direction; (2) extensive nonlinearity when loaded at 10° off-axis, and (3) relatively low strain (0.08 percent) and stress (16 ksi) to fracture in the 90° (transverse) direction. This fracture strain is only about one-fifth of that of the aluminum alloy (5 percent) and the fracture stress is about 130 percent of the corresponding stress of the aluminum (Table 2). The longitudinal fracture stress of about 180 ksi coincides with approximately 7 percent of fibers fractured (interpolated) Table 4.

The 10° off-axis stress-strain curve is shown here because it is used to determine the intralaminar shear (in-plane) stress-strain curve (Ref. 12). The result is shown in Fig. 3. It is included here to indicate the large intralaminar shear strain to fracture of about 6 percent which is several times larger than that in Fig. 2. The intralaminar shear strain at fracture is about six times greater then the "yield" shear strain of the aluminum alloy (1 percent), Table 3. The intralaminar shear stress at fracture is about 12 ksi which is about 150 percent of the shear yield stress of the aluminum alloy.

NLA stress-strain results for a $[0_2/\pm 15]_s$ APL loaded at -80° to the 0° ply direction are compared with measured data in Fig. 4. Again, the agreement is very good except for the predicted strain at fracture which is about ten times the measured value. In this case it may be considered to imply that the laminate fractured, since a relatively large strain (about 4 percent) was produced by the last load increment.

The in situ 0° ply stress-strain behavior predicted by the NLA is plotted in Fig. 5. The schematics in this figure depict the loading in the laminate, the laminate configuration, the ply orientation, and the stresses plotted. The transverse stress (σ_{122}) curve shows extensive nonlinear behavior. This stress is about 20 ksi near fracture. The corresponding strain is about 5 percent.

This 20 ksi stress is about 25 percent greater than the uniaxial value (16 ksi). The corresponding strain is about 50 times greater than the uniaxial value (0.1 percent). These comparions show significant in situ enhancement or "synergistic effect" especially for the transverse strain. The longitudinal stress (σ_{111}) is compressive and is about 40 ksi near fracture. The intralaminar shear stress (σ_{112}) is only about 2.5 ksi. Comparable in situ results for the +15° ply are shown in Fig. 6. The curves are similar for σ_{122} and σ_{111} with those of the 0° ply (Fig. 5). However, the +15° ply has an intralaminar shear stress of about 21 ksi and a corresponding strain of about 0.6 percent. The intralaminar shear stress is almost twice that of the uniaxial value (12 ksi) Fig. 3. Most of σ_{112} is due, to lamination residual stress since it remains practically constant with strain. The shear strain on the other hand is only about 10 percent of the uniaxial value. These results show that the $[0_2/\pm 15]_s$ B/A APL failed by transverse tensile ply fracture in both the 0° and +15° plies as would be expected. However, the significant in situ enhancement synergistic effect indicated by the NLA results has not been reported previously even though some part may be expected. In addition the magnitude of this "synergistic effect" can only be predicted by NLA based at the composites micromechanics level.

The 0° ply cumulative stresses are shown in Fig. 7 to illustrate the redistribution of stresses as one of the ply stresses becomes excessively

nonlinear. Note the longitudinal stress (σ_{111}) starts increasing rapidly at a laminate stress of about 14 ksi as the transverse stress (σ_{122}) approaches a horizontal tangent and therefore cannot support additional stress. The intralaminar shear stress (σ_{112}) continues to remain negligible.

NLA results are compared with measured data in Fig. 8 for the same $[0_2/\pm 15]_S$ B/AL APL but loaded at 5° to the "0" ply direction. See schematic. In this figure results are compared for axial stress (σ_{Cxx}), Poisson's strain (ϵ_{Cyy}), and "coupling shear" strain (ϵ_{Cxy}) versus axial strain (ϵ_{Cxx}). The comparisons are in very good agreement. Again, there is some discrepancy for the last load increment strain. The reason for this discrepancy is the extrapolation method used to determine the measured strain at fracture as was mentioned previously.

The in situ 0° ply stress-strain behavior predicted by the NLA is plotted in Fig. 9. As expected, the longitudinal stress (σ_{111}) dominates and reaches about 160 ksi at fracture. This approaches the uniaxial longitudinal fracture stress of 182 ksi. The other two stresses are relatively small. Corresponding stresses for the +15° ply are plotted in Fig. 10. The intralaminar shear stress (σ_{112}) starts at about -25 ksi (which is the value of lamination residual stress) and decreases to about 20 ksi. The transverse stress starts at about 10 ksi and decreases to about 5 ksi. The ply transverse strain reverses sign from initially positive (due to residual stress) to negative due to the applied stress. The in situ -15° ply stress-strain behavior is plotted in Fig. 11. The transverse stress (σ_{122}) starts at about 8 ksi (residual stress) and decreases to about 3 ksi indicating that this stress is predominantly residual. The intralaminar shear stress (σ_{112}) starts at about 17 ksi and decreases to about 10 ksi. The corresponding strains reverse sign from positive to negative. The -15° ply cumulative stresses are plotted in Fig. 12. The longitudinal stress (σ_{111}) starts from slightly negative and remains linear to fracture with increasing laminate stress. The transverse (σ_{122}) and intralaminar shear (σ_{112}) stresses vary only slightly with laminate increasing stress.

The NLA results for this laminate indicate that this laminate failed by longitudinal tension controlled mainly by fiber fractures. The other two stresses indicate negligible effect on the laminate strength.

The comparisons described previously were selected to illustrate the versatility of the NLA. In addition they were selected to illustrate laminate material nonlinear behavior, the effects of lamination residual stresses and in situ synergistic effects. Taken collectively the results show that the NLA described provides an effective analysis capability to study and determine the material nonlinear behavior of boron/aluminum APL. Such a NLA should also be applicable to metal matrix composites in general provided the required input data is available. The NLA has the capability to handle other membrane loads and bending loads and combinations. This part of the capability, however, has not as yet been validated with measured data.

Improvements to this NLA capability include local convergence, dynamic load increment and graphical display of predicted results. Additional capability includes temperature incrementation for the residual stress, fracture detection criteria, and combinations of thermal and mechanical loads incrementation and the appropriate convergence schemes.

CONCLUSIONS

A nonlinear laminate analysis (NLA) for predicting the mechanical behavior of angleplied metal matrix laminates has been formulated and programmed. The NLA was formulated using composite micromechanics, composite macromechanics, and laminate theory. This NLA allows the in situ matrix to be nonlinearily orthotropic and accounts for residual stresses, progressive fiber fractures, and relative ply rotations. Results predicted by this NLA are in excellent agreement with experimental data from boron-fiber/aluminum matrix composites except for the final strain in some cases. These results show that in situ synergistic effects enhance significantly the uniaxial composite transverse and intralaminar shear strengths. These results also show that a NLA provides an effective analysis capability to study and determine the material nonlinear behavior of metal-matrix laminates.

REFERENCES

1. Chamis, C. C., "Laminates and Reinforced Metals," NASA TM-81591, 1980.
2. Cavagnaro, D. M., "Boron Reinforced Composites, Vol. 2, A Bibliography with Abstracts," National Technical Information Service, NTIS/PS-79/0476/6, 1979.
3. Chamis, C. C. and Sullivan, T. L., "Theoretical and Experimental Investigation of the Nonlinear Behavior of Boron Aluminum Composites," NASA TM X-68205, 1973.
4. Chamis, C. C. and Sullivan, T. L., "Nonlinear Response of Boron/Aluminum Angleplied Laminates under Cyclic Tensile Loading: Contributing Mechanisms and their Effect," Fatigue of Composite Materials, ASTM STP 569, American Society for Testing and Materials, Philadelphia, 1975, pp. 95-114.
5. Chamis, C. C. and Sullivan, T. L., "A Computational Procedure to Analyze Metal Matrix Laminates with Nonlinear Lamination Residual Strains," Composite Reliability, ASTM STP 580, American Society for Testing and Materials, Philadelphia, 1975, pp. 327-339.
6. Sandhu, R. S., "Nonlinear Behavior of Unidirectional and Angle Ply Laminates," Journal of Aircraft, Vol. 13, No. 2, 1976, pp. 104-111.
7. Bahei-El-Din, Y. A., "Plastic Analysis of Metal Matrix Composite Laminates," Ph.D Dissertation, Duke University, 1979.
8. Chamis, C. C., "Computer Code for the Analysis of Multilayered Fiber Composites - User's Manual," NASA TN D-7013, 1971.
9. Wolf, J. and Brown, W. F., eds., Aerospace Structural Metals Handbook. Vol. 11, Nonferous Alloys, AFML-TR-68-115, Mechanical Properties Data Center, Traverse City, MI, 1974.
10. Chamis, C. C., Kring, J., and Sullivan, T. L., "Automated Testing Data Reduction Computer Program," NASA TM X-68050, 1972.
11. Prewo, K. M. and Kreider, K. G., "High-Strength Boron and Borsic Fiber Reinforced Aluminum," Journal of Composite Materials, Vol. 6, July 1972, pp. 338-357.
12. Chamis, C. C. and Sinclair, J. H., "Ten-deg Off-axis Test for Shear Properties in Fiber Composites," Experimental Mechanics, Vol. 17, No. 9, Sep. 1977, pp. 339-346.

TABLE 1

MATRIX PROPERTIES VS TEMPERATURE

6061-0 ALUMINUM ALLOY

TEMPERATURE, ^{o}F	MODULUS, 10^6 PSI	POISSON'S RATIO	THER COEFF EXP, 10^{-6} IN./IN./^{o}F	YIELD STRESS, PSI
0	11.3	0.310	12.1	8500
100	11.0	.330	12.8	8500
200	10.7	.350	13.5	8500
300	10.4	.345	14.1	8000
400	10.1	.335	14.7	7000
500	9.9	.330	15.2	4000
600	9.8	.330	15.8	3000
700	9.3	.330	16.5	2000
800	8.8	.345	17.2	1000
900	8.0	.350	17.9	0
1000	7.0	.350	18.6	0

TABLE 2

MATRIX STRESS/STRAIN PROPERTIES

6061-0 ALUMINUM ALLOY

STRAIN, %	STRESS, PSI	MODULUS, PSI	POISSON'S RATIO
0	0	11.0×10^6	0.366
.024	2 590	10.5	.336
.050	5 260	9.8	.334
.078	7 920	8.2	.332
.098	9 250	3.6	.392
.44	10 500	2.7×10^5	.409
1.2	11 900	8.8×10^4	.400
1.5	11 900	9.9×10^3	.397
5.0	11 900	1.0×10^1	.450

TABLE 3

MATRIX SHEAR STRESS-STRAIN PROPERTIES
6061-0 ALUMINUM ALLOY

STRAIN, %	STRESS, PSI	MODULUS, 10^6 PSI
0	0	3.27
.04	1150	3.44
.07	2450	3.57
.11	3760	3.56
.15	5090	3.32
.19	6430	2.03
.33	7810	.867
.50	8300	.100
1.00	8300	.010

TABLE 4

CUMULATIVE FIBER FRACTURE

STRESS LEVEL (KSI)	FIBERS FRACTURED (PERCENT)
200	0
250	3
300	5
350	6
400	15
450	30
475	50
500	72
525	90
530	95
550	100

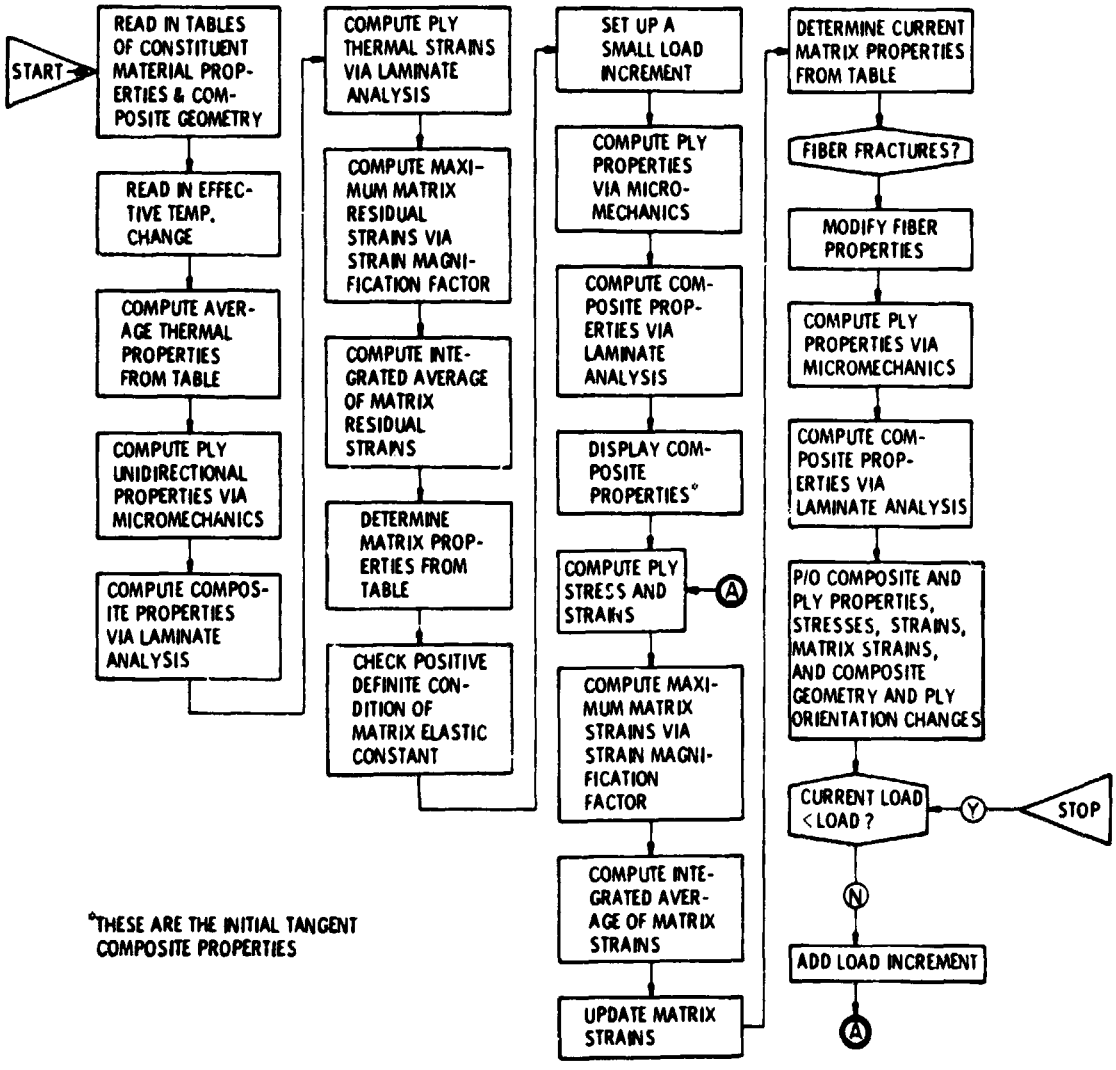

Figure 1. - Flow chart of nonlinear laminate analysis for metal matrix fiber composites.

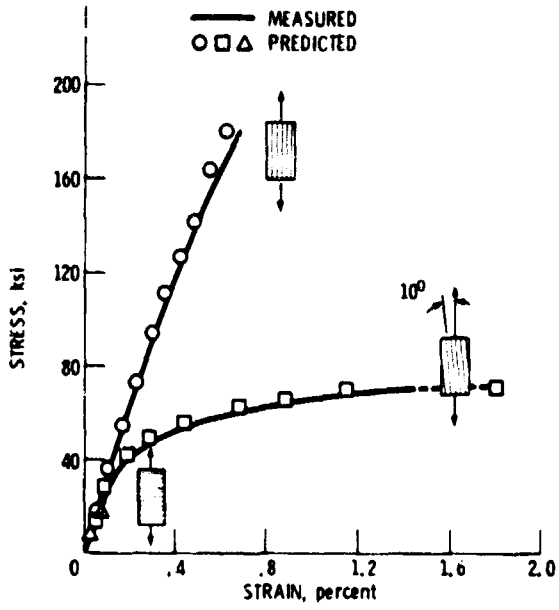

Figure 2. - Comparison of measured and predicted results. Boron/aluminum unidirectional composites. (4 mil diam. fiber, 6061-Al, 0.50 fiber volume ratio).

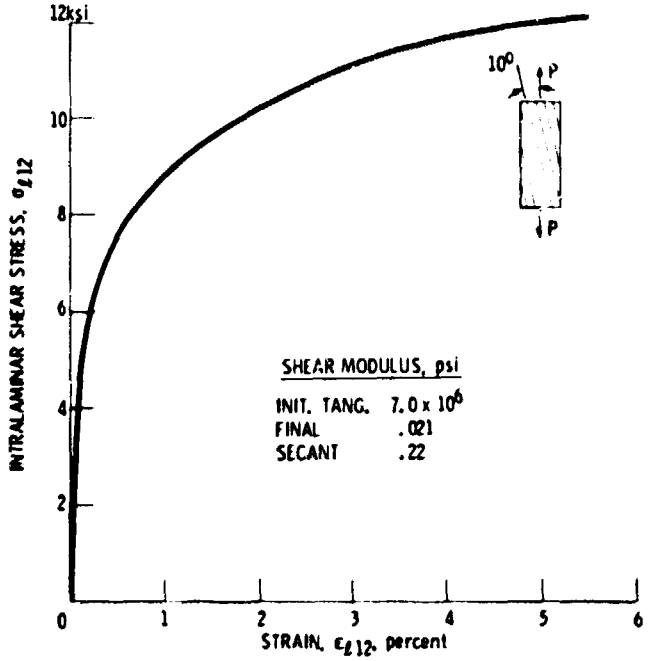

Figure 3. - Nonlinear intralaminar shear stress-strain curve of boron/aluminum.

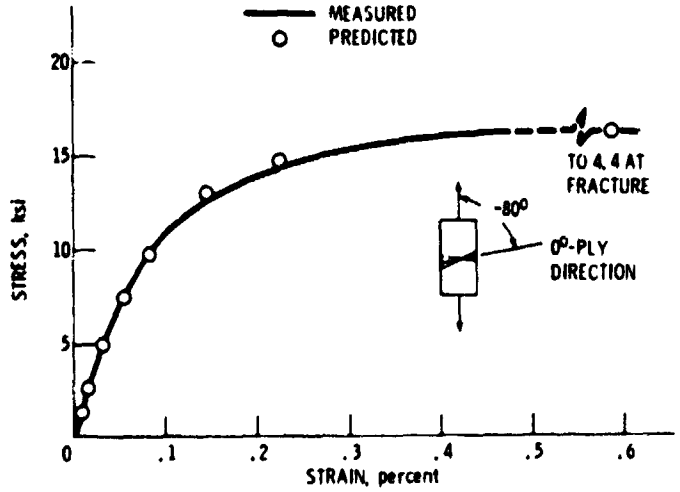

Figure 4. - Comparison of measured and predicted results. Boron/aluminum $[0_2/\pm 15]_s$ laminate loaded -80° to 0°-ply. (4 mil diam. fiber, 6061-Al, 0.50 fiber volume ratio).

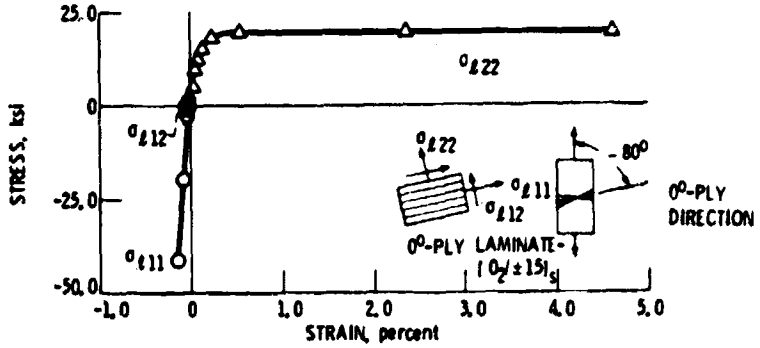

Figure 5. - 0°-ply stress-strain behavior. Boron/aluminum $[0_2/\pm 15]_s$ laminate. (4.0 mil diam. fiber, 6061-Al, 0.5 fiber volume ratio).

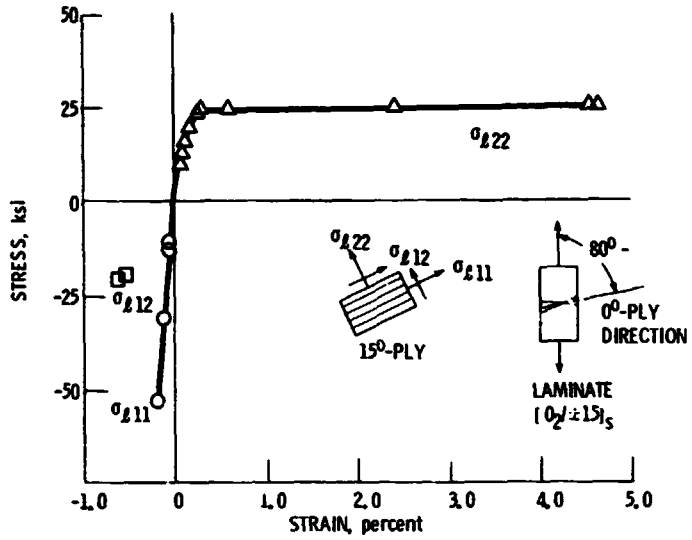

Figure 6. - 15°-ply stress-strain behavior. Boron/aluminum $[0_2/\pm 15]_S$ laminate. (4.0 mil diam. fiber, 6061-Al, 0.50 fiber volume ratio).

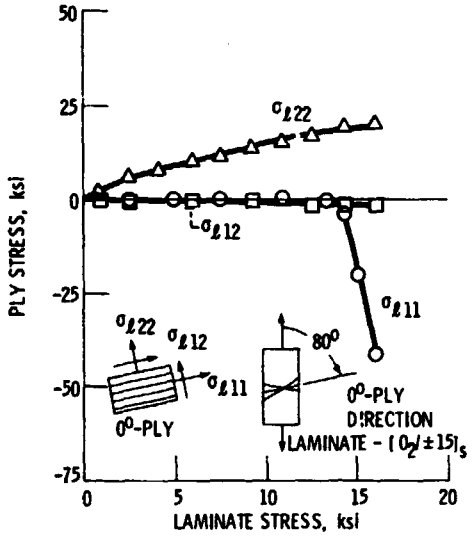

Figure 7. - 0°-ply cumulative stresses in boron/aluminum $[0_2/\pm 15]_S$ laminate. (4.0 mil diam. fiber, 6061-Al, 0.5 fiber volume ratio).

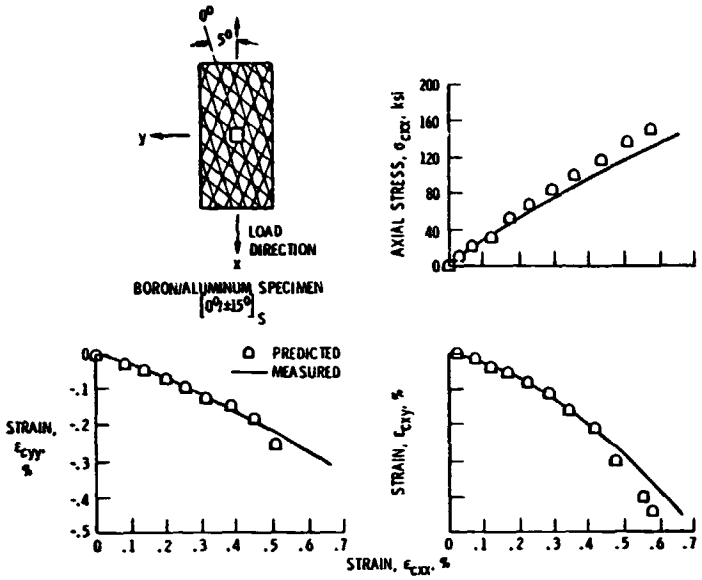

Figure 8. - Nonlinear laminate analysis results compared with measured data.

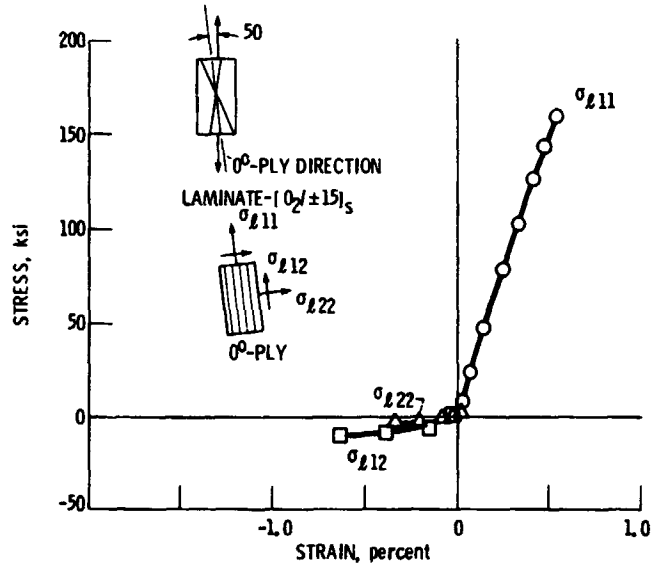

Figure 9. - 0°-ply stress-strain behavior. Boron/aluminum $[0_2/\pm 15]_S$ laminate. (4.0 mil diam. fiber, 6061-Al, 0.50 fiber volume ratio).

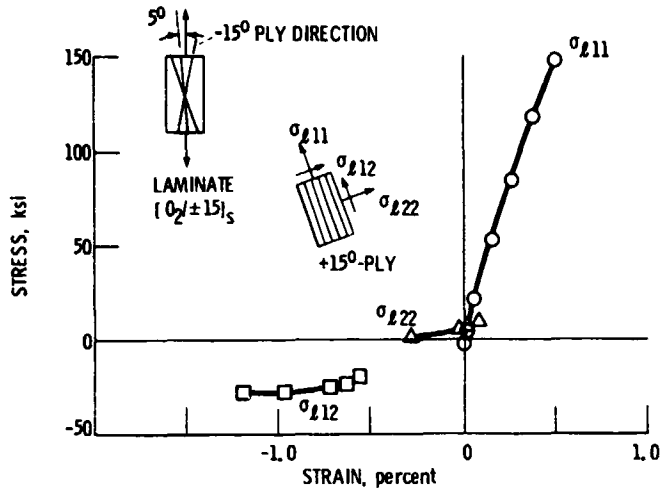

Figure 10. - 15°-ply stress-strain behavior. Boron/aluminum $[0_2/\pm 15]_s$ laminate. (4.0 mil diam. fiber, 6061-Al, 0.50 fiber volume ratio).

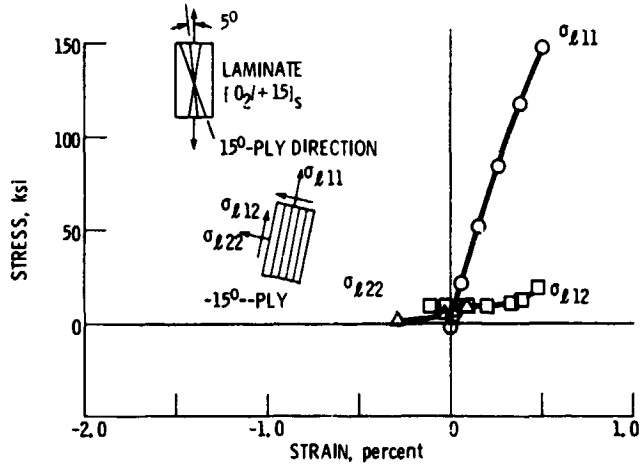

Figure 11. - 15°-ply stress-strain behavior. Boron/aluminum $[0_2/\pm 15]_s$ laminate. (4.0 mil diam. fiber, 6061-Al, 0.50 fiber volume ratio).

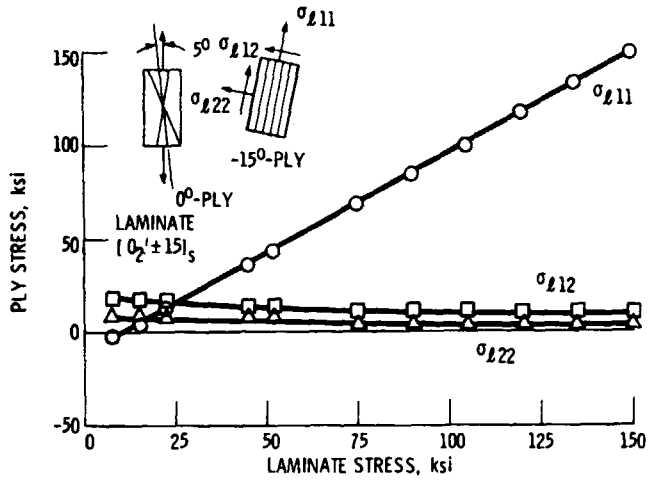

Figure 12. - 15°-ply cumulative stresses in boron/aluminum $[0_2/\pm 15]_S$ laminate. (4.0 mil diam. fiber, 6061-Al, 0.50 fiber volume ratio).